 https://doi.org/10.3311/PPch.14765

Periodica Polytechnica Chemical Engineering, 64(2), pp. 238–247, 2020

Kinetic Model of Crude Palm Oil Hydrocracking Over Ni/Mo ZrO_2–Pillared Bentonite Catalyst

Hasanudin Hasanudin[1*], Addy Rachmat[1], Muhammad Said[1], Karna Wijaya[2]

[1] Department of Chemistry, Faculty of Mathematic and Natural Science, Universitas Sriwijaya, Palembang, Sumatera Selatan 30662, Indonesia
[2] Department of Chemistry, Faculty of Mathematic and Natural Science, Universitas Gadjah Mada, Yogyakarta 55281, Indonesia
[*] Corresponding author, e-mail: hasanudin@mipa.unsri.ac.id

Received: 31 July 2019, Accepted: 05 November 2019, Published online: 17 December 2019

Abstract

Crude Palm Oil hydrocrcaking has been carried out over Ni/Mo ZrO_2–pillared bentonite catalyst in a fixed bed reactor. Crude Palm Oil hydrocracking over Ni/Mo ZrO_2–pillared bentonite catalyst formed 3 products i.e. gas, oil and coke. The oil product from Crude Palm Oil hydrocracking was analyzed by using gas chromatography to determine its composition. Three types of fraction were classified i.e. gasoline, kerosene and diesel oil. In this research, the focused of the study is of hydrocracking kinetics by using lump kinetic models. The kinetic model was solved by using the software MATLAB R2018b involves the effect of catalyst activity on the reaction rate. The results of the kinetic study show that the 4-lump (Crude Palm Oil, gas coke and oil) and 6-lump reaction models (Crude Palm Oil, gas, coke, gasoline, kerosene and diesel) can be used to explain the Crude Palm Oil hydrocracking over Ni/Mo ZrO_2–pillared bentonite catalyst. The 4-lump kinetic model has 5 rate constants and the 6-lump kinetic model has 14 rate constants.

Keywords

pillared bentonite, catalytic activity, lump reaction kinetic, hydrocracking

1 Introduction

Crude Palm Oil (CPO) obtained from extraction of palm fruit comprise of triglyceride and its free fatty acids. This vegetable oils can be converted into fuel through cracking process as reported by several authors. Among vegetable oils has been converted were oils from callophylum innophyllum seeds [1, 2], Crude Palm Oil [3-5], soybean oil [6], waste cooking oil [7-9], Rapseed oil [10] and Jatropha oil [11, 12]. Most of the products obtained from these conversion were gasoline, kerosene and diesel.

Vegetable oils conversion into fuel typically were carried out over solid catalyst i.e. transition metal embedded on a host material. There are several host materials commonly used such as zeolite, alumina and other alumina-silicate type material. Catalysts such as Mo/Al_2O_3 [13], Pd/HTlc and Ru/HTlc [11], CoMo/Alumina and NiMo/Alumina [12, 14] as well as NiMo/zeolite has been reported being used on cracking process. The most suitable catalyst concluded so far for vegetable oil hydrocracking is Ni and Mo metals [2, 3, 6, 10]. Ni/Mo ZrO_2–pillared bentonite (NMBZ) previously reported to achieve 80 % conversion on hydrocracking of remaining lipid on palm oil mill effluent [3].

Catalytic hydrocracking of triglycerides contained in vegetable oil undoubtedly involves complex reaction mechanism. The proposed mechanism so far embroils free radical formation from breaking of C-O triglyceride backbone followed by decarbonylation, decarboxylation, alkylation, cyclization, aromatization and so on. Kinetic model indispensably is important in developing hydrocracking process for large scale to obtain the most suitable parameters and to gain optimum result. Lump kinetic model has been widely used to describe process mechanism in a simple way without sacrificing the result accuracy. The application of lump kinetic model was reported in 3 and 6-lumps model [5, 15], 3 and 4-lumps model on bio-oil hydrocracking from empty fruit bunches [16] as well as 4-lumps kinetic model on hydrocracking of fresh and waste cooking oil [9, 17].

Calculation of the lump kinetics model for the hydrocracking reaction involves the catalyst deactivation process. The involvement of catalyst deactivation in this modeling is important because as long as the catalyst is used, the catalyst poisoning process occurs due to fouling,

Cite this article as: Hasanudin, H., Rachmat, A., Said, M., Wijaya, K. "Kinetic Model of Crude Palm Oil Hydrocracking Over Ni/Mo ZrO_2–Pillared Bentonite Catalyst", Periodica Polytechnica Chemical Engineering, 64(2), pp. 238–247, 2020. https://doi.org/10.3311/PPch.14765

coking, carbon deposition [18-19], poisoning [20], thermal degradation and sintering [21, 22]. All causes of deactivation are functions of time, so in this lump kinetic modeling deactivation is calculated as a function of time [21].

The number of lumped reaction used depends on several factors such as observable physical parameters, knowledge of chemical reaction involve and available kinetic data from experiments. Here, we presented 4 and 6- lumps kinetic model for Crude Palm Oil hydrocracking over NMBZ catalyst.

2 Material and methode

2.1 Material

The main material used in this work was Crude Palm Oil (CPO) obtained from Sriwijaya Palm Oil Private Company consist of major components i.e. palmitic acid (63.67 %), oleic acid (17.93 %), stearic acid (7.2 %) and linoleic acid (4.23 %) whereas catalyst was obtained from previous work [3].

2.2 Procedure

Catalytic hydrocracking reactor was setup as depicted on Fig. 1. The reactor dimension was 2.5 cm in inner diameter, 40 cm in length and 196.43 cm^3 in volume. At the beginning of the process, 12.0 g Catalyst was placed in catalyst vessel. Prior hydrocracking process, reactor was saturated by hydrogen gas to remove air at predetermined temperature for 15, minutes and flow rate 2.0 mL/sec and hydrocracking temperature varied at 673, 698, 723, 748 and 773 K. CPO was pumped in by peristaltic pump at various rate according to Weight Hourly Space Velocity (WHSV) i.e. 60, 96, 120, 150 and 300 g/hour into the preheater which then enter the gas forming reactor. The gaseous CPO formed was flowed into hydrocracking reactor driven by hydrogen in 1.0 mL/sec flow rate. Product of hydrocracking went through water cooler system and then collected in gas container. Other gas collector was arranged to capture uncondensed gas within water cooler. Coke and char deposited on catalyst were determined by gravimetric method. The reactor was washed with acetone after completing hydrocracking. The liquid product was heated in a vacuum distillation at 200 °C to obtain fractions of gasoline, kerosene and diesel oil. The remaining liquid in the flask after distillation consists of unreacted triglyceride from CPO reactant.

The liquid fractions from vacuum distillation was analyzed by using Gas Chromatography (Shimadzu, FID) to determine its composition. Three types of fraction were classified i.e. gasoline, kerosene and diesel oil.

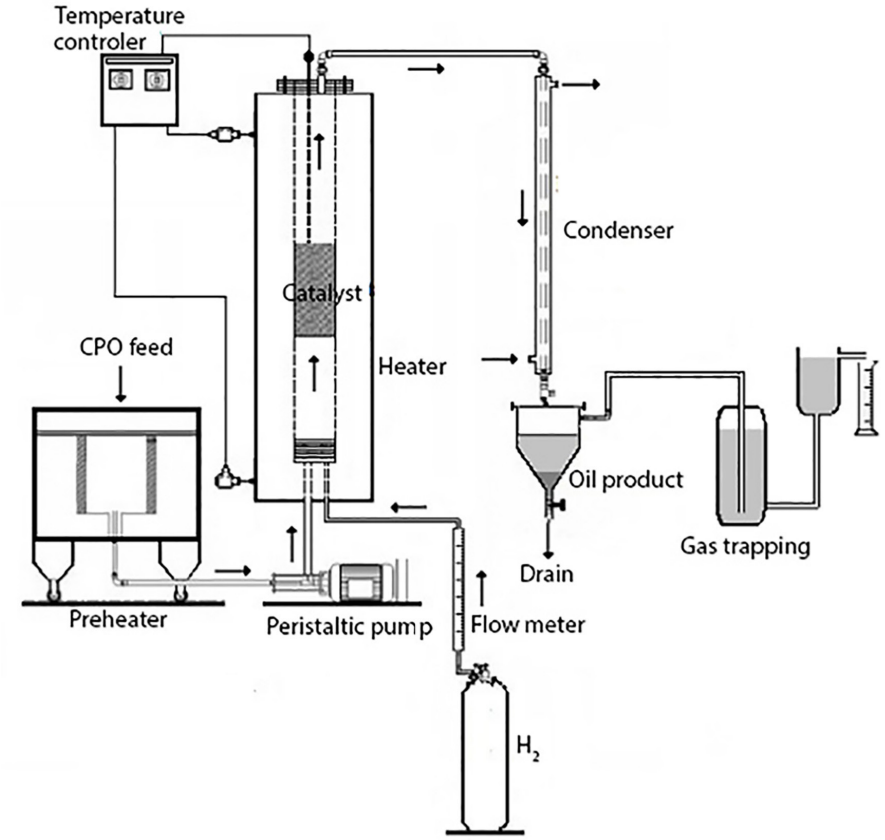

Fig. 1 Schematic diagram for catalytic hydrocracking of CPO

Data obtained were used to develop lump kinetic model. The calculation was made base on several assumptions:

1. plug-flow reactor was used;
2. axial dispersion between reactant and product is neglected;
3. all reaction proceed in first-order except for CPO feed which was presumed as second-order;
4. amount of hydrogen is insignificance compare to CPO feed hence it is pseudo-zero order with respect to hydrogen;
5. decrease on catalytic activity is a function of time of stream and temperature;
6. no coke contains in the feed;
7. water product was neglected and
8. reaction was carried out in isothermal condition.

First-order of simultaneous differential from rate equation was integrated numerically by using Runge-Kutta 4th-order equation, all of which processed in MATLAB R2018b software at initial concentration of feed $C_{CPO} = 1$ and all initial concentration of product is zero. Ode45 command was used in simultaneous integration from differential equation of rate law calculated by using Runge-Kutta 4th-order algorithm. Kinetic parameters were determined by using *F* minimize function on fminsearch command and to determine the value that gives global minimum conditions using the research step in Fig. 2 [23].

Data for kinetic parameters calculation was saved as an excel file, steps of calculation were as follows:

1. the appropriate form of rate equation was determined according to 4 and 6-reaction lumps of CPO hydrocracking by involving rate constant;
2. software will decide initial value of k which was programmed to obtain $k > 0$;
3. software calculates the value of *k* for each reactions simultaneously base on rate equation given;
4. deviation level between model calculation result and experimental data was calculated by the program as directed by Eq. (1) and
5. program adopts *k* which gave smallest SSE (Sum of Squares Errors) value where *n* is number of data.

$$\mathrm{SSE} = \sum_{i=1}^{n} \left(C_{\mathrm{calc}i} - C_{\mathrm{exp}i} \right)^2 \tag{1}$$

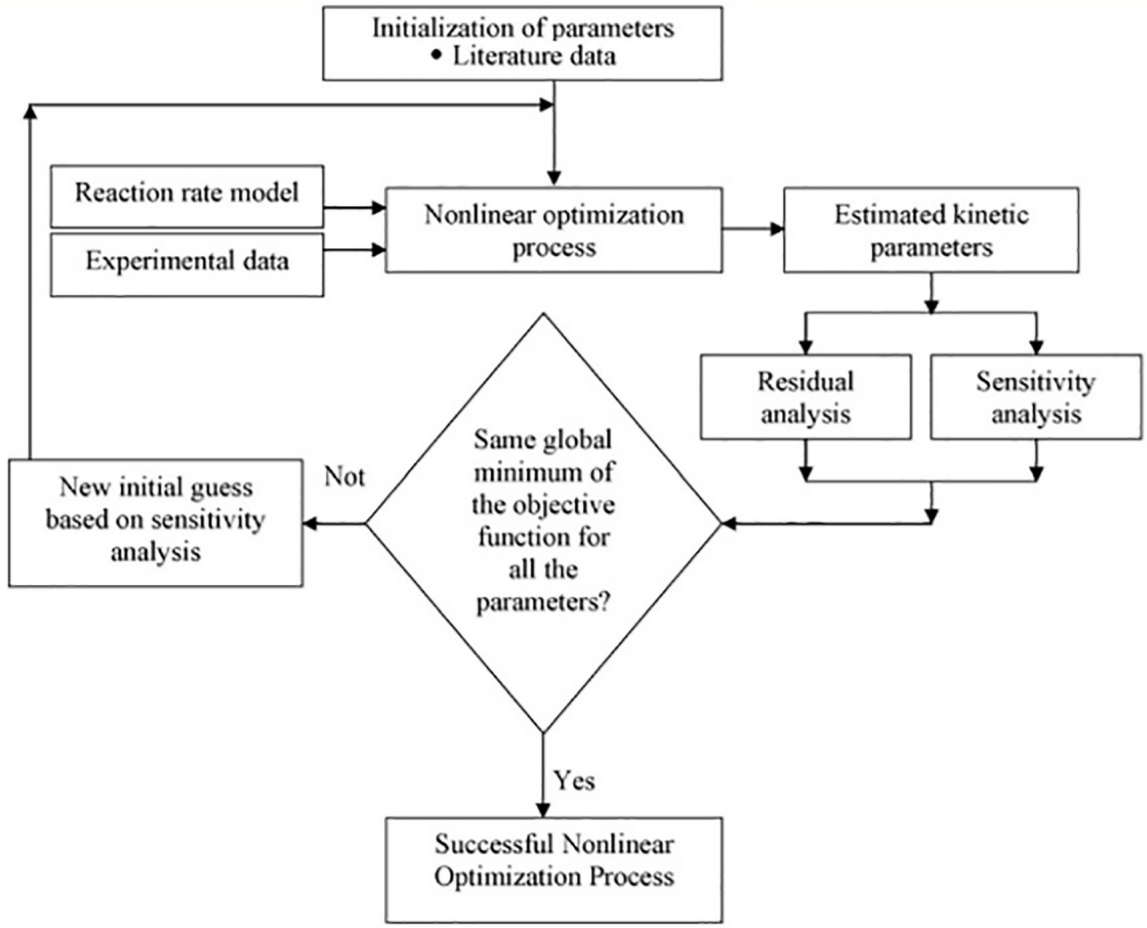

Fig. 2 Methodology for kinetic parameters estimation [23]

3 Results and discussion

3.1 Catalytic activity analysis

Catalytic activity (ϕ) is defined as ratio of reaction rate at particular time (t) to reaction rate of fresh catalyst as expressed by Eq. (2). Catalytic activity was found decreased as reaction time due to coke formation on catalyst. This phenomena is known as catalyst deactivation. Catalyst deactivation can be modelled and calculated as a function of reaction rate decrease against time.

$$\phi(t) = \frac{r_t}{r_{t=0}} \tag{2}$$

$$-\frac{d\phi}{dt} = k_d \phi^{n_i} \tag{3}$$

Some authors reported a deactivation model as a function of coke formation on catalyst surface during reaction occurrence [24-26]. Such model can be erroneous because coke formation is not the only factor involved but reaction rate and reaction time must take into account as determining variable. Deactivation model in this report was developed by calculating catalyst duration usage assuming that catalyst activity is a function of catalyst usage duration [27] and the model was formulated in Eq. (3).

Fig. 3 shows catalytic activity as well as reaction rate, decrease after t hours relative to the initial rate. The shape of the catalytic activity curve confirms a correlation of inversely proportional between activity decrease and catalyst usage duration. At short duration usage, the curve slope is steep and then become sloping. Deactivation rate equation can be solved by integrating Eq. (3) to obtain Eq. (4). Plot of ϕ_t against ln t based on Eq. (5) produced linier curve as shown on Fig. 3 having correlation coefficient (R^2) approaches 1. This linearity indicates the accuracy of deactivation rate order and constant.

$$\phi^{-n_d+1} = -k_d t\left(-n_d + 1\right) \tag{4}$$

$$\ln\phi = \frac{1}{-n_d+1}\ln\left(n_d k_d + k_d\right) + \frac{1}{-n_d+1}\ln(t) \tag{5}$$

$$n_d = 1 - \frac{1}{\text{Slope}} \tag{6}$$

$$k_d = \left(1+n_d\right)\left(e^{\text{Intercept}\left(-n_d+1\right)}\right) \tag{7}$$

Slope and intercept on Fig. 4 can be used to calculate deactivation rate order and constant by using Eqs. (6) and (7). Calculation result as shown on Table 1 concludes that deactivation rate is second-order. If the catalytic activity of fresh NMBZ equals 1 then the Eq. 4 for NMBZ

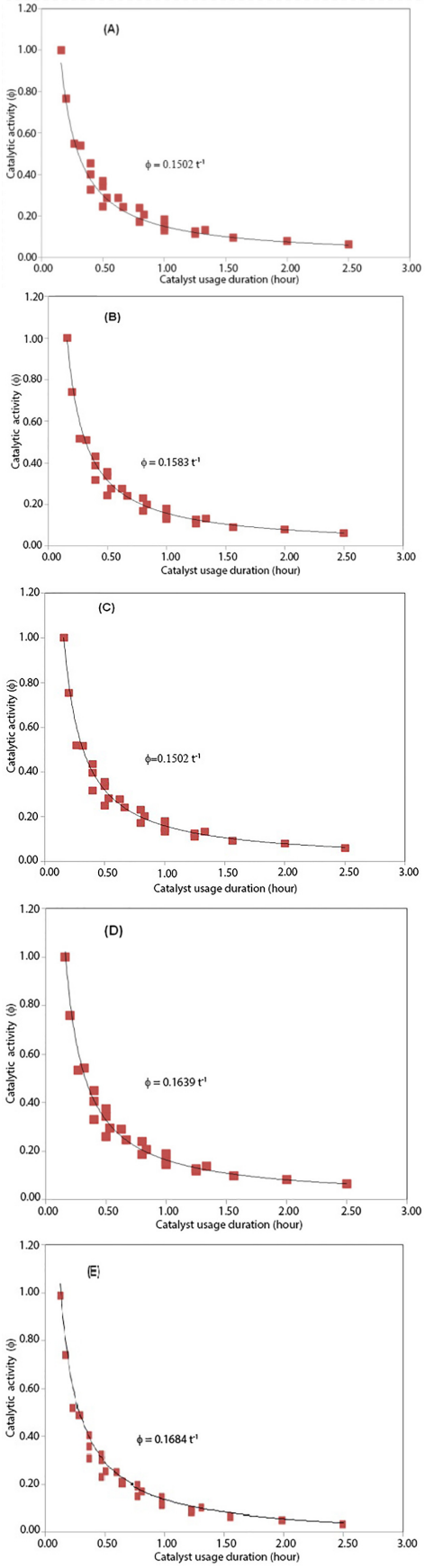

Fig. 3 The effect of catalyst usage duration on the deactivation at (A) 673 K, (B) 698 K, (C) 723 K, (D) 748 K and (E) 773 K

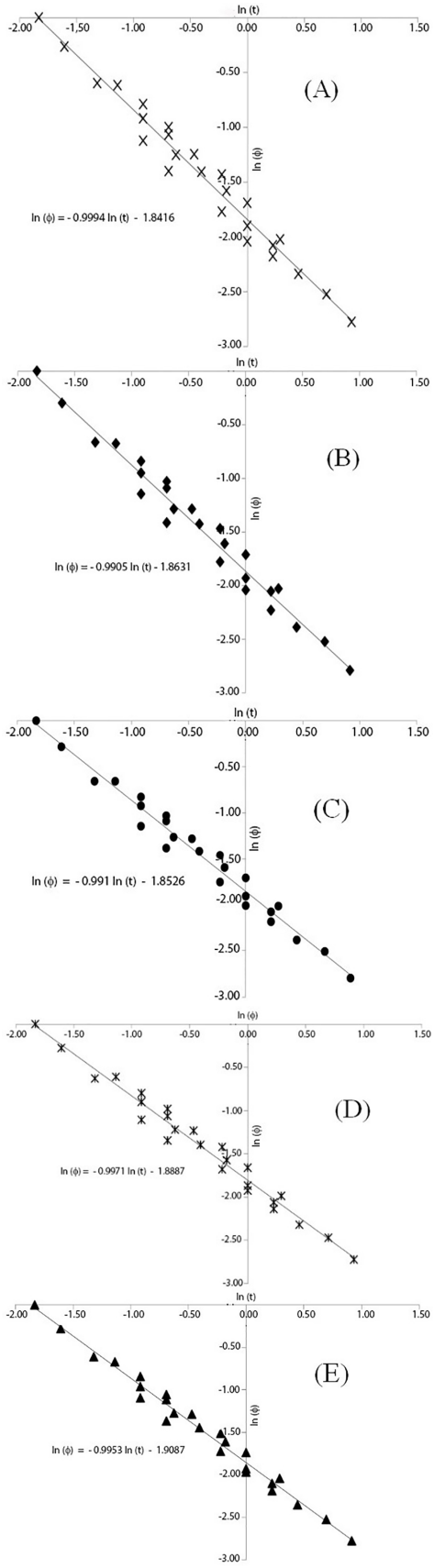

Fig. 4 Relationship between ln (t) vs ln (ϕ) at (A) 673 K, (B) 698 K, (C) 723 K, (D) 748 K and (E) 773 K

Tabel 1 Deactivation rate order (n_d) and constant (k_d) at various reaction temperature

Temperature (K)	n_d	k_d
673	2.01	18.92
698	2.01	19.39
723	2.00	19.55
748	2.00	19.85
773	2.00	20.26

catalytic activity on CPO hydrocracking becomes Eq. (8). Furthermore, deactivation rate constant is highly affected by hydrocracking temperature, the higher temperature used, constant of deactivation also becomes larger. Catalyst tend to deactivate rapidly which then shorten its lifetime at high temperature.

$$\phi = \left(k_d t\right)^{-1} \tag{8}$$

Effect of temperature on deactivation process can be describe by applying Arrhenius equation. Application of Arrhenius equation was carried out by using deactivation rate constant and temperature on Table 1 which will give frequency factor (A) and deactivation energy (E_d). The result for A and E_d are 2.75×10^{12} and 54.27 kJ K^{-1} mol^{-1} respectively.

3.1.1 4-Lump reaction kinetic model

Lump reaction kinetic model was used in this report to solve equation for complex reaction of hydrocracking over NMBZ catalyst. CPO cracking has been reported in 3-lump (Fig. 5) reaction kinetic model by several authors [5, 15]. This model however has weakness on merging gas and coke into one lump reaction even though their display different property. In the process, gas leaves reactor along with oil whereas coke forms solid product. The coke later becomes major cause for catalyst deactivation.

The 3-lump reaction model drawback can be improved by separating gaseous product and coke into different lumps. First step in this kinetic study of CPO hydrocracking over NMBZ catalyst is by proposing 4-lumps as depicted in Fig. 6. According to this model, CPO hydrocracking

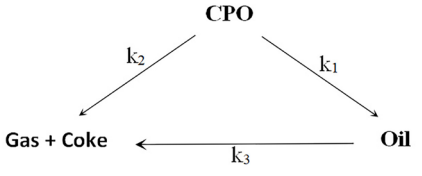

Fig. 5 Kinetic model by using 3-lump reaction for CPO cracking [5, 15]

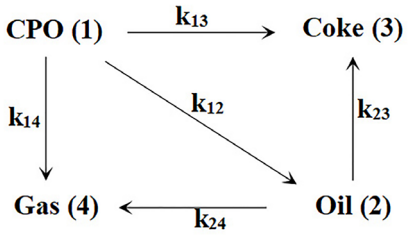

Fig. 6 Kinetic model by using 4-lump reaction for CPO cracking

formed 3 products i.e. gas, oil and coke each of with its own rate constant k_{14}, k_{12} and k_{13}. The oil can be cracked further to forms gas and coke having rate constants k_{24} and k_{23} respectively. Calculation of rate equation by involving catalyst activity were formulated by Eqs. (9)-(12).

$$\frac{dC_{\text{CPO}}}{d\tau} = -\phi\left(k_{12} + k_{13} + k_{14}\right)C_{\text{CPO}}^{n} \tag{9}$$

$$\frac{dC_{\text{Oil}}}{d\tau} = \phi\left(k_{12}C_{\text{CPO}}^{n} - \left(k_{23} + k_{24}\right)C_{\text{Oil}}^{n}\right) \tag{10}$$

$$\frac{dC_{\text{Coke}}}{d\tau} = \phi\left(k_{13}C_{\text{CPO}}^{n} + k_{23}C_{\text{Oil}}^{n}\right) \tag{11}$$

$$\frac{dC_{\text{Gas}}}{d\tau} = \phi\left(k_{14}C_{\text{CPO}}^{n} + k_{24}C_{\text{Oil}}^{n}\right) \tag{12}$$

Equations (9)-(12) are hard to solve due to unknown reaction order. The solution to this equation can be obtained by making assumption such as reactant was reacted in a complex reaction having second order against the main reactant. Reaction which occurs further is regarded as elementary reaction having first-order in rate. These assumptions has been used by several authors to solve reaction rate of crude oil cracking [28-29]. Applying the assumptions, Eqs. (9)-(12) can be written into Eqs. (13)-(16).

$$\frac{dC_{\text{CPO}}}{d\tau} = -\phi\left(k_{12} + k_{13} + k_{14}\right)C_{\text{CPO}}^{2} \tag{13}$$

$$\frac{dC_{\text{Oil}}}{d\tau} = \phi\left(k_{12}C_{\text{CPO}}^{2} - \left(k_{23} + k_{24}\right)C_{\text{Oil}}\right) \tag{14}$$

$$\frac{dC_{\text{Coke}}}{d\tau} = \phi\left(k_{13}C_{\text{CPO}}^{2} + k_{23}C_{\text{Oil}}\right) \tag{15}$$

$$\frac{dC_{\text{Gas}}}{d\tau} = \phi\left(k_{14}C_{\text{CPO}}^{2} + k_{24}C_{\text{Oil}}\right) \tag{16}$$

MATLAB R2018b software was used to conduct calculation and the rate constants for 4-lumps kinetic model result are shown on Table 2. The result shows k_{12} relatively bigger than other rate constants which means the hydrocracking reaction was dominated by oil formation followed by gas and coke. By using this k value, catalyst selectivity to produce oil, gas, coke and ratio needed in further oil cracking were formulated in Eqs. (17)-(19).

Table 2 Rate constants of CPO hydrocracking using 4-lump reaction model

	Rate constants				
k_{ij}	673 K	698 K	723 K	748 K	773 K
k_{12}	1.2610	2.6321	3.4738	3.4738	3.7736
k_{13}	0.0602	0.3273	0.7874	0.8008	1.1910
k_{14}	1.2112	1.6006	2.1154	2.1701	2.7237
k_{23}	0.0991	0.4139	0.5006	0.5594	0.6041
k_{24}	0.3181	0.6736	0.7874	0.9332	1.2889

$$S_{\text{Oil}} = \frac{k_{12}}{k_{13} + k_{14}} \tag{17}$$

$$S_{\text{Coke}} = \frac{k_{13}}{k_{12} + k_{14}} \tag{18}$$

$$S_{\text{Gas}} = \frac{k_{14}}{k_{12} + k_{13}} \tag{19}$$

$$P_{\text{Oil}} = \frac{k_{23} + k_{24}}{k_{12} + k_{13} + k_{14}} \tag{20}$$

Equations (17)-(20) were used to analyze the selectivity and ratio of further hydrocracking reaction of CPO feed over NMBZ catalyst. The calculation result is shown on Figs. 7 and 8. Catalyst selectivity on oil product is in the range of 0.45–0.58. The selectivity is increased by temperature from 0.45 at 673 K to 0.56 at 698 K.

The catalyst selectivity in hydrocracking process to produce oil is relatively constant between 0.56–0.58 at 698 K. The further hydrocracking process on the oil produced provide this constant selectivity. The aforementioned

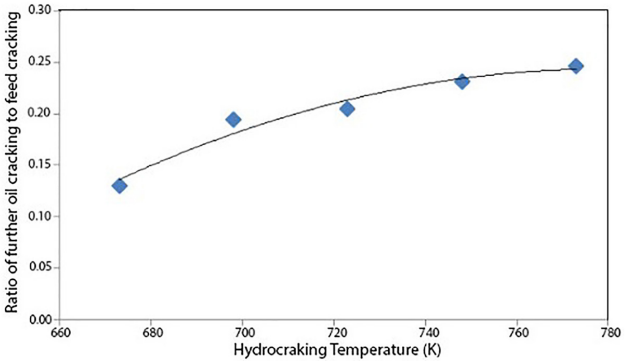

Fig. 7 Selectivity against oil, coke and gas in CPO hydrocracking products over NMBZ catalyst

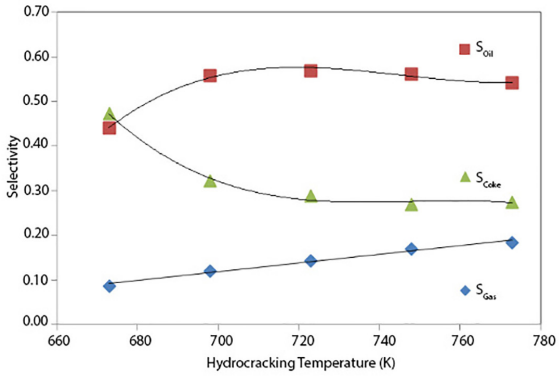

Fig. 8 The oil product to feed ratio on CPO hydrocracking

hydrocracking produced gas and some coke. At higher temperature, further hydrocracking reaction produced gas caused catalyst selectivity on oil product to decrease. The increase ratio of oil product from further hydrocracking against CPO hydrocracking provide indication of selectivity decrease. Selectivity and cracking ratio are considered good if it has value between 0.63–90 and 0.00–0.09 [24]. This work obtained selectivity and ratio at 0.45–0.58 and 0.10–0.25 respectively.

Rate constant at various temperature can be used to calculate frequency factors and activation energies of particular reaction. Arrhenius equation was used in the calculation and the result is shown on Table 3. Based on Table 3, the formation reaction of oil from CPO has the highest activation energy compared to the formation of coke and gas. Although the activation energy of oil formation from CPO is greatest, the rate constant of the formation of oil from CPO is highest so that the rate of formation of oil remains the highest so the selectivity of oil formation is also the highest.

3.2 6-Lump kinetic model

Rate equation commonly includes all compounds involves in the reaction (both reactant and product). Hydrocracking is a complex reaction with so many compounds produced during reaction hence it is almost impossible to do a complete calculation. Lump kinetic model designed to solve such reaction by making several assumptions. The more numbers of lumps used, the better kinetic model obtained due to smaller error on compound characters grouping in a single lump. Therefore, the 4-lump kinetic model was further developed by expanding to 6-lumps reaction. These lumps comprise of lump 1 (CPO), lump 3 (coke) and lump 4 (gas) as in 4-lumps model. Lump 2 (oil product) was break down into lump 5 (diesel fraction), lump 6 (kerosene fraction) and lump 7 (gasoline fraction). The reaction scheme of 6-lumps CPO hydrocracking is shown on Fig. 9.

$$\frac{dC_1}{d\tau} = -\phi\left(k_{13} + k_{14} + k_{15} + k_{16} + k_{17}\right)C_1^2 \quad (21)$$

$$\frac{dC_7}{d\tau} = \phi\left(k_{17}C_1^2 + k_{57}C_5 + k_{67}C_6 - k_{73}C_7 - k_{74}C_7\right) \quad (22)$$

$$\frac{dC_5}{d\tau} = \phi\left(k_{15}C_1^2 - k_{53}C_5 - k_{56}C_5 - k_{54}C_5 - k_{56}C_5 - k_{57}C_5\right) \quad (23)$$

$$\frac{dC_6}{d\tau} = \phi\left(k_{16}C_1^2 + k_{56}C_5 - k_{63}C_6 - k_{64}C_6 - k_{67}C_6\right) \quad (24)$$

$$\frac{dC_3}{d\tau} = \phi\left(k_{13}C_1^2 + k_{53}C_5 + k_{63}C_6 + k_{73}C_7\right) \quad (25)$$

$$\frac{dC_4}{d\tau} = \phi\left(k_{14}C_1^2 + k_{54}C_5 + k_{64}C_6 + k_{74}C_7\right) \quad (26)$$

Rate law for this 6-lump reaction as depicted on Fig. 9 was formulated by Eqs. (21)-(26). Gasoline fraction was produced from hydrocracking of CPO, diesel and kerosene fraction as formulated in Eq. (22). The gasoline however, can be further break down to form gas product. Kerosene was formed from CPO and diesel fraction hydrocracking whereas diesel was obtained only from CPO hydrocracking. Three fractions (gasoline, kerosene and diesel) can undergo cracking process to form gas and coke. Rate equation for coke formation from gas will gave rate constant k_{GC} as reported by Twaiq et al. [5]. Here, we did not use such assumption i.e. coke formation from gas. The formation of coke generally was initiated from aromatic compounds which undergo further reaction and released hydrogen to form naphthalene. Naphthalene is

Table 3 The frequency factor and activation energy of 4-lump reaction model on CPO hydrocracking

Reaction			A	E_a (kJ K^{-1} mol^{-1})
CPO	→	Oil	1.2610	2.6321
CPO	→	Coke	0.0602	0.3273
CPO	→	Gas	1.2112	1.6006
Oil	→	Coke	0.0991	0.4139
Oil	→	Gas	0.3181	0.6736

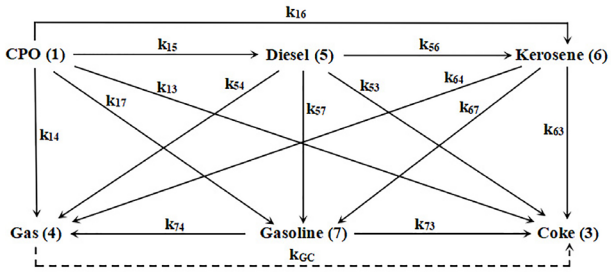

Fig. 9 6-lump kinetic model of CPO hydrocracking

hard to diffuse out from catalyst hence it will forms coke on catalyst surface [29].

Data experiment processing base on Eqs. (19)-(24) by using MATLAB R2018b was able to obtain rate constants for 6-lump kinetic model of CPO hydrocracking over NMBZ catalyst as did Twaiq et al. [5] by using Polymath software. Two different software does not means result in difference rate constants, but different assumptions used evidently result in different rate constants as shown by our result and Twaiq et al. [5]. Rate constants for coke and gas formation was obtained from 4-lump model and stated as k_{13} and k_{14}. These constants were adopted from 4-lump model and used in 6-lump model of CPO hydrocracking. The 6-lump kinetic model produced 14 rate constants including 2 which was calculated from 4-lump model and the result is shown on Table 4. Back to Table 4, k_{15} relatively bigger than any other rate constants. Triglyceride hydrocracking according to the table was dominated by formation of diesel fraction, but data shows gasoline fraction formed in larger amount then diesel. Kinetic model in 6-lump reaction provide reason that the diesel fraction produced only from triglyceride hydrocracking. Gasoline fraction has more source of formation i.e. hydrocracking of triglyceride, diesel and kerosene fraction. Diesel fraction in chemical structure point of view has number of C-atom almost similar to triglyceride reactant hence this product is not hard to form by hydrocracking reaction.

The effect of temperature on hydrocracking process was evaluated according to Arrhenius equation by using deactivation rate constant and temperature displayed on Table 4. The calculation provide linier curve whilst the frequency factor (A) and activation energy (E_a) is shown on Table 5. The main difference between our results with previous report by Twaiq et al. [5] lays on coke formation from gas product as described earlier. Activation energy for this process as reported by this author has negative value hence it is reasonable that this report assumed no formation of coke from gas hydrocracking product.

Validation test for 6-lump reaction kinetic model is displays on Fig. 10. The regression constant calculated shows value close to 1 which means this model with 14 rate

Table 4 Rate constant for 6-lump kinetic model of CPO hydrocracking

	Rate constants					
k_{ij}	673 K	698 K	723 K	748 K	773 K	723 K*
k_{14}	0.0602	0.3273	0.7874	0.8008	1.1910	0.1150
k_{14}	1.2112	1.6006	2.1154	2.1701	2.7237	0.2500
k_{15}	0.5477	1.1397	1.7404	1.9150	2.5153	1.522
k_{16}	0.4024	0.7138	0.8265	1.3323	1.8205	0.6520
k_{17}	0.1866	0.3761	0.4725	0.5846	0.8564	0.9388
k_{53}	0.1064	0.2027	0.1839	0.3922	0.5087	0.3600
k_{54}	0.0027	0.0031	0.0099	0.0893	0.1088	0.9105
k_{56}	0.0237	0.0513	0.0616	0.1055	0.1273	1.5220
k_{57}	0.0156	0.0267	0.0696	0.0850	0.1118	0.1328
k_{63}	0.1066	0.1471	0.1709	0.3333	0.4322	0.0000
k_{64}	0.1184	0.1289	0.1878	0.2839	0.4169	0.0000
k_{67}	0.0188	0.0368	0.0598	0.2550	0.4908	0.0000
k_{73}	0.0953	0.1302	0.1642	0.1820	0.2741	0.2000
k_{74}	0.0058	0.0169	0.0308	0.0945	0.1261	0.0000
k_{GC}	-	-	-	-	-	0.0606

Note: *Twaiq et al. [5] used polymath software

Table 5 Frequency factor and activation energy based on 6-lump reaction model for CPO hydrocracking

Reaction			A	E_a (kJ K^{-1} mol^{-1})	A^*	E_a^* (kJ K^{-1} mol^{-1})
CPO	→	Coke	0.06	0.33	4.39×10^{8}	132.19
CPO	→	Gas	1.21	1.60	1.46×10^{20}	287.16
CPO	→	Diesel	4.62×10^{4}	62.42	7.18×10^{11}	162.95
CPO	→	Kerosene	3.32×10^{4}	63.08	2.38×10^{12}	175.59
CPO	→	Gasoline	1.10×10^{4}	60.69	5.31×10^{12}	178.75
Diesel	→	Coke	1.32×10^{4}	65.45	1.86×10^{12}	176.92
Diesel	→	Gas	4.14×10^{11}	185.53	1.07×10^{13}	179.58
Diesel	→	Kerosene	8.88×10^{3}	71.08	1.78×10^{9}	125.79
Diesel	→	Gasoline	1.31×10^{5}	88.76	5.36×10^{8}	132.44
Kerosene	→	Coke	6.71×10^{3}	62.27	1	0.00
Kerosene	→	Gas	2.62×10^{3}	56.77	1	0.00
Kerosene	→	Gasoline	3.12×10^{9}	145.77	1	0.00
Gasoline	→	Coke	1.83×10^{2}	42.27	1.39×10^{21}	304.70
Gasoline	→	Gas	2.67×10^{8}	136.89	1	0.00
Gas	→	Coke	-	-	2.52×10^{-10}	−115.23

Note: *Twaiq et al. [5] data was calculated by using Polymath software

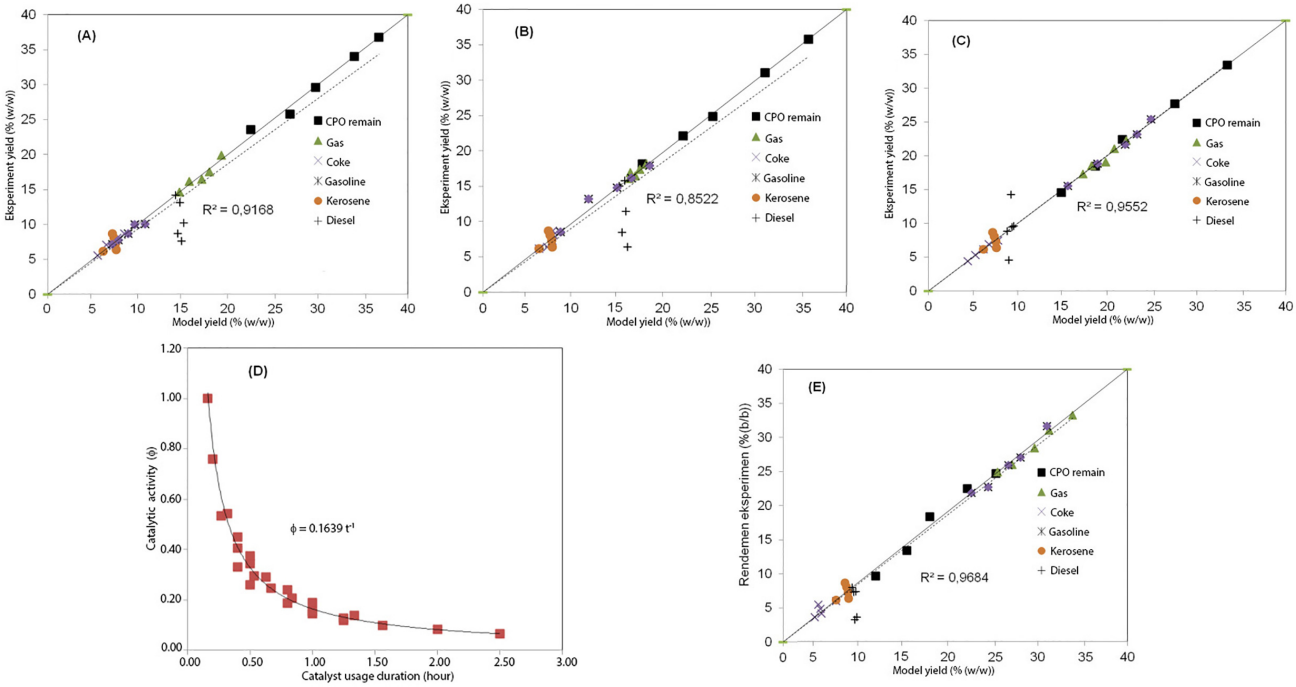

Fig. 10 Gas yield and triglyceride remain according to experiment and 6-lump kinetic model calculation at (A) 673 K, (B) 698 K, (C) 723 K, (D) 748 K and (E) 773 K

constants (k_{13}, k_{14}, k_{15}, k_{16}, k_{17}, k_{53}, k_{54}, k_{56}, k_{57}, k_{63}, k_{64}, k_{67}, k_{73} and k_{74}) can be accepted to describe triglyceride hydrocracking over NMBZ catalyst.

4 Conclusion

Kinetic model base on 4 and 6-lumps reaction was developed to describe CPO hydrocracking over NMBZ catalyst. The model was validated and fit with experimental data as represented by regression linear constant. The activity of catalyst in this model is a function of time and temperature. The longer hydrocracking time and the higher temperature caused decrease of NMBZ activity. Reaction models by using 4 and 6-lumps proved its accuracy on describing reaction kinetic of CPO hydrocracking over NMBZ catalyst.

Acknowledgement

This work is supported by Sriwijaya University, through Hibah Kompetitif 2019.

References

[1] Dewajani, H., Rochmadi, Purwono, S., Budiman, A. "Kinetic Study of Catalitic Cracking of Indonesian Nyamplung Oils (*Calophyllum inophyllum*) over ZSM-5 Catalyst", ARPN Journal of Engeering and Applied Sciences, 11(8), pp. 5221–5226, 2016. [online] Available at: https://pdfs.semanticscholar.org/b0df/9398b67e03f15d62659745cf44b0539d4a06.pdf [Accessed: 12 June 2019]

[2] Savitri, Effendi, R., Tursiloadi, S. "Cracking vegetable oil from *Callophyllum innophyllum L.* seeds to bio-gasoline by Ni-Mo/Al_2O_3 and Ni-Mo/Zeolite as micro-porous catalysts", In: 2nd Padjadjaran International Physics Symposium, Bandung, Indonesia, 2016, Article number: 050008. https://doi.org/10.1063/1.4941891

[3] Hasanudin, H., Said, M. H., Faizal, M., Dahlan, M. H., Wijaya, K. "Hydrocracking of oil residue from palm oil mill effluent to biofuel", Sustainable Environment Research, 22(6), pp. 395–400, 2012.

[4] Bhatia, S., Mohamed, A. R., Shah, N. A. A. "Composites as cracking catalysts in the production of biofuel from palm oil: Deactivation studies", Chemical Engineering Journal, 155(1–2), pp. 347–354, 2009. https://doi.org/10.1016/j.cej.2009.07.020

[5] Twaiq, F., Mohamed, A. R., Bhatia, S. "Catalytic Cracking of Palm Oil Into Liquid Fuels: Kinetic Study", In: Proceedings Of The Seventh Asia-Pacific International Symposium on Combustion and Energy Utilization (7th APISCEU), Hong Kong, China, 2004, pp. 1–8. [online] Available at: http://eprints.usm.my/id/eprint/14296 [Accessed: 10 August 2018]

[6] Ishihara, A., Fukui, N., Nasu, H., Hashimoto, T. "Hydrocracking of soybean oil using zeolite–alumina composite supported NiMo catalysts", Fuel, 134, pp. 611–617, 2014. https://doi.org/10.1016/J.FUEL.2014.06.004

[7] Hanafi, S. A., Elmelawy, M. S., Shalaby, N. H., El-Syed, H. A., Eshaq, G., Mostafa, M. S. "Hydrocracking of waste chicken fat as a cost effective feedstock for renewable fuel production: A kinetic study", Egyptian Journal of Petroleum, 25(4), pp. 531–537, 2016. https://doi.org/10.1016/J.EJPE.2015.11.006

[8] Wako, F. M., Reshad, A. S., Bhalerao, M. S., Goud, V. V. "Catalytic cracking of waste cooking oil for biofuel production using zirconium oxide catalyst", Industrial Crops and Products, 118, pp. 282–289, 2018. https://doi.org/10.1016/j.indcrop.2018.03.057

[9] Periyasamy, B. "Reaction pathway analysis in thermal cracking of waste cooking oil to hydrocarbons based on monomolecular lumped kinetics", Fuel, 158, pp. 479–487, 2015. https://doi.org/10.1016/J.FUEL.2015.05.066

[10] Sotelo-Boyás, R., Liu, Y., Minowa, T. "Renewable Diesel Production From the Hydrotreating of Rapeseed Oil with Pt/Zeolite and NiMo/Al_2O_3 Catalysts", Industrial & Engineering Chemistry Research, 50(5), pp. 2791–2799, 2011. https://doi.org/10.1021/ie100824d

[11] Patil, S. J., Vaidya, P. D. "On the production of bio-hydrogenated diesel over hydrotalcite-like supported palladium and ruthenium catalysts", Fuel Processing Technology, 169, pp. 142–149, 2018. https://doi.org/10.1016/J.FUPROC.2017.09.026

[12] Patil, S. J., Vaidya, P. D. "Production of Hydrotreated Jatropha Oil Using Co–Mo and Ni–Mo Catalysts and Its Blending with Petroleum Diesel", Energy & Fuels, 32(2), pp. 1812–1821, 2018. https://doi.org/10.1021/acs.energyfuels.7b03305

[13] Hossain, M. Z., Chowdhury, M. B. I, Jhawar, A. K., Xu, W. Z., Biesinger, M. C., Charpentier, P. A. "Continuous Hydrothermal Decarboxylation of Fatty Acids and Their Derivatives into Liquid Hydrocarbons Using Mo/Al_2O_3 Catalyst", ACS Omega, 3(6), pp. 7046–7060, 2018. https://doi.org/10.1021/acsomega.8b00562

[14] Kumar, P., Maity, S. K., Shee, D. "Role of NiMo Alloy and Ni Species in the Performance of NiMo/Alumina Catalysts for Hydrodeoxygenation of Stearic Acid: A Kinetic Study", ACS Omega, 4(2), pp. 2833–2843, 2019. https://doi.org/10.1021/acsomega.8b03592

[15] Yared, I., Kurniawan, H., Wibisono, N., Sudaryanto, Y., Hindarso, H., Ismadji, S. "Modeling of Liquid Hydrocarbon Fuel Production from Palm Oil via Catalytic Cracking Using MCM-41 as Catalyst", ARPN Journal of Engineering and Applied Science, 2(3), pp. 55–62, 2008. [online] Available at: https://www.arpnjournals.com/jeas/research_papers/rp_2008/jeas_0408_95.pdf [Accessed: 12 June 2019]

[16] Sunarno, S., Rochmadi, R., Mulyono, P., Aziz, M., Budiman, A. "Kinetic Study of Catalytic Cracking of Bio-Oil over Silica-alumina Catalyst", BioResources, 13(1), pp. 1917–1929, 2018. https://doi.org/10.15376/biores.13.1.1917-1929

[17] Meier, H. F., Wiggers, V. R., Zonta, G. R., Scharf, D. R., Simionatto, E. L., Ender, L. "A kinetic model for thermal cracking of waste cooking oil based on chemical lumps", Fuel, 144, pp. 50–59, 2015. https://doi.org/10.1016/j.fuel.2014.12.020

[18] Cordero-Lanzac, T., Aguayo, A. T., Gayubo, A. G., Costaño, P., Bilbao, J. "Simultaneous modeling of the kinetics for n-pentane cracking and the deactivation of a HZSM-5 based catalyst", Chemical Engineering Journal, 331, pp. 818–830, 2018. https://doi.org/10.1016/j.cej.2017.08.106

[19] Tirado, A., Ancheyta, J., Trejo, F. "Kinetic and Reactor Modeling of Catalytic Hydrotreatment of Vegetables Oils", Energy & Fuels, 32(7), pp. 7245–7261, 2018. https://doi.org/10.1021/acs.energyfuels.8b00947

[20] Albers, P., Pietsch, J., Parker, S. F. "Poisoning and deactivation of palladium catalysts", Journal of Molecular Catalysis A: Chemical, 173(1–2), pp. 275–286, 2001. https://doi.org/10.1016/S1381-1169(01)00154-6

[21] Argyle, M. D., Bartholomew, C. H. "Heterogeneous Catalyst Deactivation and Regeneration: A Review", Catalysts, 5(1), pp. 145–269, 2015. https://doi.org/10.3390/catal5010145

[22] Bartholomew, C. H. "Mechanisms of catalyst deactivation", Applied Catalysis A: General, 212(1–2), pp. 17–60, 2001. https://doi.org/10.1016/S0926-860X(00)00843-7

[23] Acharya, D. R., Hughes, R., Li, K. "Deactivation of silica-alumina catalyst during the cumene cracking reaction", Applied Catalysis, 52(1), pp. 115–129, 1989. https://doi.org/10.1016/S0166-9834(00)83376-X

[24] Forrissier, M., Formenti, M., Bernard, J. R. "Effect of total preasure on catalytic cracking reaction", Catalysis Today, 11(1), pp. 73–83, 1991. https://doi.org/10.1016/0920-5861(91)87008-B

[25] Pitualt, I., Nevicato, D., Foressier, M., Bernard, J. R. "Kinetic model based on a molecular description for catalytic cracking of vacuum gas oil", Chemical Engineering Science, 49(24), pp. 4249–4262, 1994. https://doi.org/10.1016/S0009-2509(05)80018-1

[26] Corma, A., Wojciechowski, B. W. "The Chemistry of Catalytic Cracking", Catalysis Reviews Science and Engineering, 27(1), pp. 29–150, 1985. https://doi.org/10.1080/01614948509342358

[27] Ruszkowski, M. F., Gomzi, Z., Tomić, T. "4-LUMP Kinetic Model for Hydrotreated Gas Oil Catalytic Cracking", Chemical and Biochemical Engineering Quarterly, 20(1), pp. 61–68, 2006.

[28] Ancheyta-Juárez, J., López-Isunza, F., Aguilar-Rodríguez, E. "5-Lump kinetic model for gas oil catalytic cracking", Applied Catalysis A: General, 177(2), pp. 227–235, 1999. https://doi.org/10.1016/S0926-860X(98)00262-2

[29] Benson, T. J., Hernandez, R., French, W. T., Alley, E. G., Holmes, W. E. "Elucidation of the catalytic pathway for unsaturated mono-, di-, and triacylglycerides on solid acid catalysts", Journal of Molecule Catalysis A: Chemical, 303(1–2), pp. 117–123, 2009. https://doi.org/10.1016/j.molcata.2009.01.008